The Conduction of Protons in Different Stereoisomers of Dioxolane-Linked Gramicidin A Channels

Edward P. Quigley,* Paulene Quigley,# David S. Crumrine,# and Samuel Cukierman*
*Department of Physiology, Loyola University Medical Center, and #Department of Chemistry, Loyola University Chicago, Maywood, Illinois 60153 USA

ABSTRACT Two different stereoisomers of the dioxolane-linked gramicidin A (gA) channels were individually synthesized (the SS and RR dimers; Stankovic et al., 1989. *Science.* 244:813–817). The structural differences between these dimers arise from different chiralities within the dioxolane linker. The SS dimer mimics the helicity and the inter- and intramolecular hydrogen bonding of the monomer-monomer association of gA's. In contrast, there is a significant disruption of the helicity and hydrogen bonding pattern of the ion channel in the RR dimer. Single ion channels formed by the SS and RR dimers in planar lipid bilayers have different proton transport properties. The lipid environment in which the different dimers are reconstituted also has significant effects on single-channel proton conductance (g_H). g_H in the SS dimer is about 2–4 times as large as in the RR. In phospholipid bilayers with 1 M $[H^+]_{bulk}$, the current-voltage (*I-V*) relationship of the SS dimer is sublinear. Under identical experimental conditions, the *I-V* plot of the RR dimer is supralinear (S-shaped). In glycerylmonooleate bilayers with 1 M $[H^+]_{bulk}$, both the SS and RR dimers have a supralinear *I-V* plot. Consistent with results previously published (Cukierman et al., 1997. *Biophys. J.* 73:2489–2502), the SS dimer is stable in lipid bilayers and has fast closures. In contrast, the open state of the RR channel has closed states that can last a few seconds, and the channel eventually inactivates into a closed state in either phospholipid or glycerylmonooleate bilayers. It is concluded that the water dynamics inside the pore as related to proton wire transfer is significantly different in the RR and SS dimers. Different physical mechanisms that could account for this hypothesis are discussed. The gating of the synthetic gA dimers seems to depend on the conformation of the dioxolane link between gA's. The experimental results provide an important framework for a detailed investigation at the atomic level of proton conduction in different and relatively simple ion channel structures.

INTRODUCTION

The transfer of protons in proteins and across biological membranes is an essential phenomenon in biology (Deamer and Nichols, 1989; DeCoursey and Cherny, 1994, 1999; Oliver and Deamer, 1994). ATP production is triggered by proton transfer in membrane proteins. Chains of water molecules and proton shuttle by amino acids in energy transducing enzymes have been demonstrated in the photosynthetic reaction center (Baciou and Michel, 1995), and in cytochrome *c* oxidase (Riistma et al., 1997), respectively. Despite its central role in life, the essential mechanisms underlying protein-assisted proton flow are not completely understood. Because gramicidin A (gA) is a water-filled ion channel pore with a proton conductance that can easily be measured (Akeson and Deamer, 1991; Cukierman et al., 1997; Eisenman et al., 1980; Heinemann, 1990; Hladky and Haydon, 1972; Levitt and Decker, 1988; Myers and Haydon, 1972), this ion channel has been used in both experimental and theoretical fronts as a model to promote our understanding of the basic rules of proton transport in proteins (Akeson and Deamer, 1991; Cukierman et al., 1997; Phillips et al., 1999; Pomès and Roux, 1996).

gA is a pentadecapeptide secreted by *Bacillus brevis*. Its unusual alternating sequence of D and L amino acids determines a $\beta^{6.3}$ helix structure in different molecular environments (Arseniev et al., 1985; Ketchem et al., 1993). In lipid bilayers, six intermolecular H-bonds are established between the amino termini of two gA's, resulting in the formation of an ion channel that is selective for monovalent cations only. Disruption of these H-bonds destabilizes the ion channel, leading to its disappearance. In 1989, Stankovic et al. developed an ingenious strategy for covalently linking two gA monomers. Using a dioxolane ring that allows a continuous and constrained transition between the two β helices of gA's, those authors demonstrated that the covalently linked gA dimer formed ion channels in lipid bilayers. As anticipated, covalently linked gA channels had lifetimes considerably longer than that of the monomer-monomer association of gA's via H-bonds. Because tartaric acid is the starting compound in the synthesis of the dioxolane linker, two stereochemically different dioxolane-linked gA dimers were synthesized in the dimerization process of gA's: the SS and the RR dimers (Stankovic et al., 1989). There are several advantages in using the dioxolane-linked gA's to study proton currents in proteins. One of them is the possibility of introducing discrete changes in the polarity or stereochemistry of the dioxolane linker (Stankovic et al., 1989, 1990; Cukierman et al., 1997). Because these molecular changes do not hamper the formation of ion channels in

Received for publication 16 March 1999 and in final form 22 June 1999.
Address reprint requests to Dr. Samuel Cukierman, Department of Physiology, Loyola University Medical Center, 2160 South First Avenue, Maywood, IL 60153. Tel.: 708-216-9471; Fax: 708-216-6308; E-mail: scukier@luc.edu.

0006-3495/99/11/2479/13 $2.00

planar lipid bilayers, the structure-function relationships in a relatively simple protein can then be studied in relation to proton flow.

Previous work from our laboratory has determined the single-channel proton conduction and gating (opening and closing of the channel) in dioxolane-linked gA's in different lipid environments (Cukierman et al., 1997; Quigley et al., 1998). A racemic mixture of tartaric acid was used in our initial chemical synthesis, leading to the formation of both the SS and the RR dioxolane-linked gA dimers. It was not possible to separate these different dimers by conventional purification procedures. Consequently, our previous single-channel experiments in lipid bilayers with the product of the dimerization reaction revealed the presence of different channels with open state durations considerably longer than those of conventional gA channels. Unfortunately, it was not possible to unequivocally correlate the structure of each dimer (RR or SS) with its functional characteristics in lipid bilayers. Parenthetically, this illustrates the significant theoretical difficulties confronting the elucidation of the precise relationship between structure and function in ion channels. Even when the structure of a "simple" ion channel is relatively well known, as is the case with gA channels, it is very difficult, if not impossible at present, to predict the function of an ion channel from its structure and vice versa (Koeppe and Andersen, 1996).

Our interest in the basic mechanisms of proton conduction in proteins prompted the synthesis of each of the dioxolane-linked gA stereoisomers individually. To this end, the chemical synthesis of linked gA's started with the SS or RR tartaric acids (Stankovic et al., 1989, 1990). In this study, the resulting SS or RR gA dimers were studied individually in different lipid bilayers in HCl solutions. Significant differences in single-channel gating and proton conductances were found between these two different dioxolane-linked dimers. We have now concluded that the previously characterized D_1 dimer (Cukierman et al., 1997; Quigley et al., 1998) is indeed the SS stereoisomer of the dioxolane-linked gramicidin A channel. Moreover, our experimental results suggest that differences in single-channel proton currents between the SS and RR dimers must be caused by differences in water dynamics inside the pores of these channels (Cukierman et al., 1997; Pomès and Roux, 1996; Quigley et al., 1998). In turn, this must reflect appreciable changes in H-bond energetics between water molecules inside the channel and carbonyl groups lining the pore of the SS or RR gA dimers.

MATERIALS AND METHODS

Synthesis and purification of different gA dimers

Dioxolane-linked gA dimers were prepared in three consecutive steps. First, the SS or RR stereospecific dioxolane dicarboxylic acids were synthesized from D-diethyl ester tartrate and L-diethyl ester tartrate, respectively. The diethyl ester protecting groups were removed, and the diacids were purified for further reactions. Second, natural gA was desformylated and purified. Third, the dioxolanes were coupled to two deprotected gA's and purified for biophysical studies.

The SS dioxolane linking reagent was prepared from the corresponding D-diethyl tartrate ester (Stankovic et al., 1989, 1990) .The diethyl tartrate was refluxed neat with diethoxymethane and catalytic *p*-toluenesulfonic acid under argon for 24–48 h at 95°C. The intermediate bis ethoxymethyl diester was converted to the closed ring under slow distillation at 105–115°C until no diethoxymethane or ethanol was collected. The remaining dioxolane diethyl ester was separated from *p*-TsOH and unreacted diethyl tartrate by silica gel chromatography. Thin-layer chromatography and H-NMR were utilized to determine fractions containing dioxolane-linked diester without unreacted diethyl tartrate. The dioxolane diester was saponified with 1 M NaOH for 90 min. Neutralization, acidification, and extraction with diethyl ether followed. The aqueous fraction was concentrated and triturated with ethyl acetate to yield the SS dioxolane dicarboxylic acid.

In parallel to the production of the respective dioxolane dicarboxylic acid stereoisomers, desformylated gA was prepared and purified. In contrast to our previous studies (Cukierman et al., 1997; Quigley et al., 1998), in which gA was purified by large-scale flash chromatography from the natural mixture of gramicidins A, B, and C, the current syntheses utilized purified gA from Fluka (Milwaukee, WI). This gA was desformylated and used in both the SS and RR synthesis. gA was desformylated by anhydrous hydrogen chloride (acetyl chloride in methanol, 2.9 M), with stirring for 60 min at room temperature. The reaction mixture was concentrated, dissolved in glacial acetic acid, and lyophilized for 24 h. Desformyl gA was separated from unreacted gA on a water-jacketed Ag11A8 column (1×50 cm), eluted with MeOH and 2 N NH_4OH in MeOH. Desformyl gA purity was further enhanced by preparative high-performance liquid chromatography (HPLC) on a reverse-phase C18 column, using methanol/water (Waters Co., Milford, MA).

The respective SS or RR linking reagent was covalently attached to two deprotected gA's via a diphenylphosphorylazide-mediated coupling in dimethyl formamide at −20°C for 48–96 h with catalytic triethylamine (15%). The reaction was quenched with MeOH and lyophilized. This crude product was purified by preparative HPLC on reverse-phase C18 with isocratic 95/5 MeOH/H_2O at 1.5 ml/min. The dimer fractions from multiple runs were pooled, concentrated, and repurified by HPLC to minimize gA contamination. Between purifications of either stereoisomer of the dimers, the injector, tubing, column, and detector were flushed extensively.

It is important to discuss the possibility of different products from the dimerization reaction. 1) Commercially available gA (Fluka, Milwaukee, WI) was used for the synthesis of the RR or SS dimers. The contamination of gramicidin C (gC) or B (gB) in that sample was very low. In our previous studies (Cukierman et al., 1997; Quigley et al., 1998), gA was purified from gB and gC by flash chromatography. The purity of these different gA samples was assessed by thin-layer chromatography and reverse-phase HPLC. Even if small amounts of gC or gB had remained throughout the synthesis reaction, the possibility of heterodimer (gA-gB, gA-gC) or homodimer (gB-gB, gC-gC) formation would certainly not have occurred in significant yields. Moreover, heterodimers have different retention times, and were not detected by the photodiode array of the HPLC. 2) The stability of gA was high under different phases of synthesis purification. Tryptophan degradation did not occur over the time course of dimer synthesis and purification. 3) The respective SS and RR dioxolane diethyl ester was separated by column chromatography from unreacted diethyl tartrate. The RR and SS linking reagents were assessed before and after removal of the ester protecting group for the continued presence of the closed dioxolane ring. Thus it is not likely that the ring hydrolyzed during the dimerization reaction. 4) It could be argued that a desformyl gA and a half-reacted SS or RR dioxolane-gA monomer form ion channels in lipid bilayers. However, desformyl gA was removed by ion exchange chromatography and further purified by HPLC. Desformyl gA and gA eluted before gA dimers. Therefore, it is not likely that the two components of these potential asymmetrical heterodimers would have been present in the bilayer set-up in significant amounts. In conclusion, our bilayer results with channels with very long open times, in relation to natural gA channels, suggest that those are indeed the SS and RR dioxolane-linked dimers.

NMR characterization

Proton NMR (Varian VXR400 or Varian VXR300) was used to characterize the individual linking reagents and the gA dimers. Two singlets appeared for the dioxolane link at 5.25 (s, 2H) and 4.75 (s, 2H), corresponding to the methylene protons of the dioxolane ring and the proton on the chiral carbons.

Molecular modeling of gA dimers

Molecular models of the SS and RR dioxolane-linked gramicidin dimers were developed using Insight and CHARMm 22 and manipulated using WebLab Viewer Pro (these three different software packages were from Molecular Simulations, San Diego, CA). Gramicidin A coordinates were retrieved from the Brookhaven Protein Data Bank (access code 1grm). The two stereospecific linking reagents were produced. Gramicidin A was digitally desformylated, and the respective linking reagent was docked into the space created by deletion of the two N-terminal valines. Models with the dioxolane group facing into the channel were constructed from the previous models by nearly symmetrical distortion of the amino acids near the linker, rotation of the dioxolane ring, and then attempting to restore helicity and continuity of the lumen by allowed rotations (peptide bond torsions or isomerizations were not attempted). For the purposes of these models, the dioxolane ring was treated as a rigid entity.

Characterization of ion channels in lipid bilayers

Experimental procedures were the same as before (Cukierman et al., 1997; Quigley et al., 1998). Briefly, membranes were formed onto a 0.1-mm-diameter hole in a polystyrene cup (*cis* side) nested inside a plastic chamber that formed the *trans* side. Membranes had the following compositions: 1) PEPC 4:1 (60 mM in decane), 1-palmitoyl-2-oleoyl-phosphatidylethanolamine (PE), and 1-palmitoyl-2-oleoyl-phosphatidylcholine (PC); 2) glycerylmonooleate (GMO) (60 mM in decane). Phospholipids were obtained from Avanti Lipids (Alabaster, AL), and GMO was from NuCheck (Elysian, MN). Experiments were performed at room temperature (21–23°C).

Both sides of the membrane were connected to an Axopatch 1D amplifier (Axon Instruments, Foster City, CA) via Ag/AgCl wires immersed in solutions. Two different voltage-clamp protocols were applied across the lipid bilayers: 1) a steady DC voltage (range: 0–400 mV) was used, and 2) in PEPC bilayers, voltage clamp ramps from 0 to 380 mV were generated in ~7.5 s. Because GMO bilayers are far less stable at high voltages than PEPC bilayers, voltage ramps from 0 to ~200–250 mV were used in the former. The single-channel recordings shown in this study are representative of typical experiments. The SS and RR dimers each have consistent and reproducible electrophysiological characteristics that are easily identifiable during a bilayer experiment by their relatively long open durations, shapes of the single-channel current-voltage relationships, and their single-channel conductances. In this paper, *n* is the number of different channels recorded in different lipid bilayers of a given composition.

In the experimental conditions of this study (low pH), PE and PC are protonated. Consequently, PEPC bilayers are positively charged. In contrast, GMO membranes are neutral. To compare proton concentrations in different GMO or PEPC bilayers as seen by the channel openings, the concentration of protons at the PEPC-membrane/solution interface ($[H^+]_{x=0}$) was calculated using a model based on the Gouy-Chapman-Stern model (Cukierman, 1991; Cukierman et al., 1997). This calculation rests on several assumptions that may not be entirely correct. One of these assumptions relates to the pK of phospholipid protonation in the lipid bilayer. Not only is this value unknown, but it is expected that pK shifts as phospholipids become protonated. Therefore, calculations of $[H^+]_{x=0}$ must be understood as a first rough approximation for the proton concentration at the membrane/solution interface.

RESULTS

In this section, some structural differences between the SS and RR dimers that are relevant for proton conduction in gA dimer channels will be presented (Figs. 1 and 2, and Table 1). A description of the functional differences between proton conduction and gating in the SS versus RR dimers in different experimental conditions will follow (Figs. 3–8, and Table 2).

Fig. 1 shows an inside-the-pore view of the dioxolane group (identified by carbons in *yellow*) connecting two gA molecules. Only the three central loops from the β-helix are shown in this figure: the central loop, and those immediately above (Val_7, *upper left*), and below (Val'_7—the prime identifies a residue in a different gA monomer—*lower left*) that central loop. The left and right panels represent the SS and RR dimers, respectively. H-bonds in this figure are represented by yellow dashed lines. In natural gA, three symmetrical pairs of H-bonds stabilize the formation of an ion channel in the bilayer ($Val_1 \rightarrow Ala'_5$; $Ala'_5 \rightarrow Val_1$; $Ala_3 \rightarrow Ala'_3$). This H-bonding motif continues along the peptide, leading to a $\beta^{6.3}$ helix. Deletion of the formyl groups and covalent attachment of the SS dioxolane linker do not significantly distort the dipeptide (Stankovic et al., 1989). This is consistent with the previous functional finding that proton conduction in the SS is similar to natural gA in lipid bilayers (Cukierman et al., 1997). The two carbonyls of the dicarboxylic acid replace the formyl groups, allowing the same intrastrand hydrogen bonds with Val^7. In both panels of Fig. 1 the dioxolane ring is facing away from the lumen of the pore.

Significant structural differences were noted between the SS and RR linked dimers. The change in chirality from SS to RR creates distortion between the two gA monomers, disrupting interstrand hydrogen bonding. Note the significant difference in the pitch of the dioxolane ring between the SS and RR dimers in Fig. 1. The C_2-C_3 bonds of the SS and RR dioxolane rings differ by ~95° relative to each other. Whereas in the SS dimer the dioxolane ring is parallel to the plane of the bilayer, in the RR it is nearly perpendicular to the plane of the bilayer. Because of differences in chirality at the linking reagent, distortions of the peptide backbone were noticed in the RR in relation to the SS dimer.

To better understand the alterations of secondary structure in the two stereospecific dimers, the geometries of H-bonds were examined as markers of carbonyl and amino orientation. Table 1 lists the unique inter- and intrastrand hydrogen bonds from the dioxolane linker to the C terminus. The parameters given are the H $\rightarrow$O distance, the N-H $\rightarrow$ O donor angle, the CO $\leftarrow$ H acceptor angle, and the torsion between donor and acceptor. Column 1 lists the hydrogen bonds in order of amino donor to carbonyl acceptor, starting from the center of the channel and radiating outward for a single monomer only. Several differences in H-bonding between the SS and RR linked gramicidin dimers are noteworthy. There was some variability in the H $\rightarrow$ O distances as also documented by Crouzy et al. (1994), and one H-

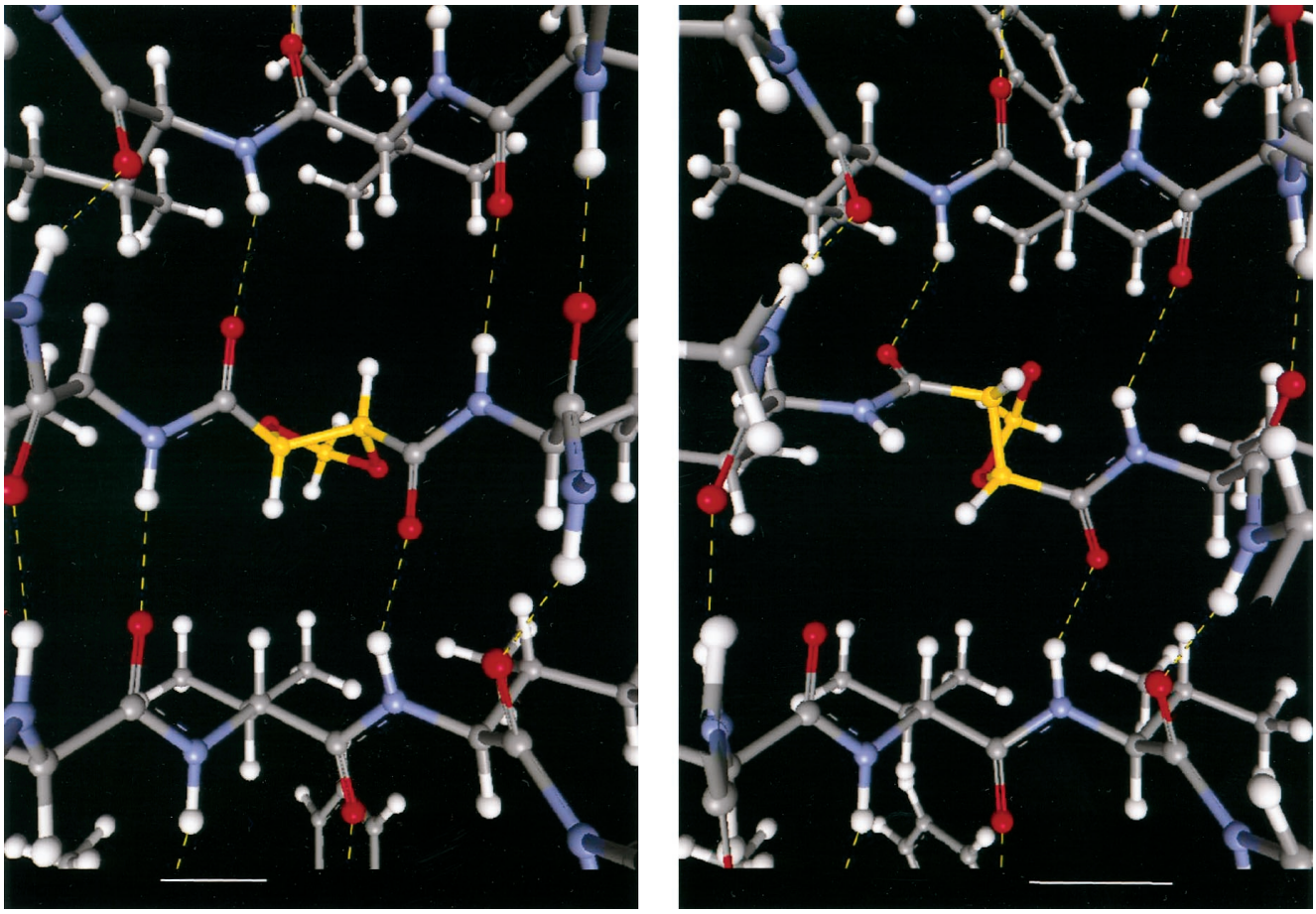

FIGURE 1 Close-up at the dioxolane linker in the SS (*left*) and RR (*right*) dimers as viewed from inside the lumen of the channel. H-bonds are indicated in yellow dashed lines. See text and Table 1 for a detailed discussion of the figure. Calibration bars at the bottom of the panels represent 2.5 Å.

bond ($Val'^{1} \rightarrow Ala^{5}$) was not formed in the RR dimer because of the pronounced tilt about the dioxolane link. This tilt increased the distance between the donor H (in Val'^{1}) to the acceptor O (in Ala^{5}) from 1.95 Å in the SS to 3.56 Å in the RR, eliminating the H-bond in the latter. Some changes were also noticed in the donor and acceptor angles as well

TABLE 1 Geometry of H-bonds in the SS and RR dimers

H-bond*	Distance (Å)[#] SS/RR	Angle (°)[§] SS/RR	Angle (°)[¶] SS/RR	Torsion (°)[‖] SS/RR
$Ala'^{3} \rightarrow Ala^{3}$**	2.37/2.10	128.7/134.0	142.5/136.9	83.5/68.7
$Ala^{5} \rightarrow Val'^{1}$	1.89/2.09	159.7/160.3	160.0/153.8	−22.0/−102.9
$Val'^{1} \rightarrow Ala^{5}$	2.18/no	152.6/no	173.7/no	114.9/no
$Val^{7} \rightarrow$ dioxolane	2.06/1.81	146.9/144.0	170.2/122.7	119.5/38.4
$Gly^{2} \rightarrow Val^{7}$	1.87/1.85	158.4/163.4	141.4/139.9	−83.9/−117.3
$Trp^{9} \rightarrow Gly^{2}$	2.22/2.28	138.8/138.3	116.5/130.0	−44.5/−50.0
$Leu^{4} \rightarrow Trp^{9}$	2.07/2.17	144.4/150.7	141.4/151.2	78.7/71.3
$Trp^{11} \rightarrow Leu^{4}$	2.09/2.07	138.1/164.3	145.8/159.7	13.6/25.9
$Val^{6} \rightarrow Trp^{11}$	2.12/2.18	147.5/150.1	142.0/148.2	−53.6/−39.0
$Trp^{13} \rightarrow Val^{6}$	2.06/2.08	150.5/156.6	148.6/170.3	−31.9/−91.2
$Trp^{15} \rightarrow Val^{8}$	2.09/2.33	162.8/150.6	158.6/148.5	−3.9/17.4
$Leu^{10} \rightarrow Trp^{15}$	2.18/1.89	144.6/151.5	120.5/142.8	18.1/−35.2

*Arrows indicate direction of the H-bond (from amino to carbonyl).
[#]Shortest distance in Å between the H and O.
[§]Angle measured between NH and O.
[¶]Angle measured between CO and H.
[‖]Torsional angle between NH and CO.
**Prime denotes H-bonds between different gA monomers.

TABLE 2 Single-channel proton conductances of RR and SS dimers under different experimental conditions*

Experimental conditions	RR	SS
PEPC, 1 M HCl	232 ± 4 pS (23)	509 ± 8 (13)
GMO, 1 M HCl	353 ± 10 pS (5)	856 ± 10 (6)
GMO, 0.122 M HCl	47 ± 2 pS (12)	189 ± 9 pS (4)

*Mean ± SEM (number of channels in different bilayers).

as torsion between the SS and RR. Because of some asymmetry in the distortion, only one of the pairs of Val'^{1} to Ala^{5} was lost. The planes of some of the peptide bonds, which are generally perpendicular to the plane of the bilayer in the SS dimer, become tilted in the RR linked gA. This results in an increased pitch and tilt of the amino and carbonyl groups. This initial survey does not take into account peptide bond isomerization or carbonyl polarity. But it does demonstrate that even a subtle chirality change can cause significant alterations in protein secondary structural motifs (Crouzy et al., 1994). These structural differences between the SS and RR dimers are likely to be relevant for proton conduction through the pore. Because water molecules inside the channel interact electrostatically with the wall of the channel (Pomès and Roux, 1996), a change in the geometries of the peptide carbonyls can cause differences in water-peptide interactions. In turn, this may have a significant impact on proton transfer along the pore (see Discussion).

Fig. 2 shows cross-sectional views of the pore of the SS (*upper row*) and RR (*lower row*) dimers. Molecular dynamic simulations by Crouzy et al. (1994), in which dimer closures were caused by rotation of the dioxolane linker inside the channel lumen (Stankovic et al., 1989, 1990), prompted the models of the SS and RR dimers with the dioxolane linker protruding inside the pore. The right panels in Fig. 2 show the SS and RR dimers with the lumen partially obstructed by the dioxolane linker. In Fig. 2, O is represented by red, N by blue, hydrogens are omitted, and the dioxolane carbons are yellow. The white bar in each panel is 3 Å. The panels to the left show the same structures as seen in Fig. 1 (with the dioxolane ring pointing away from the pore). In the upper left panel, the orientation of the SS dioxolane is parallel to the plane of the bilayer and perpendicular to the barrel of peptide and hydrogen bonds. In the lower left panel, note that the pitch of the RR

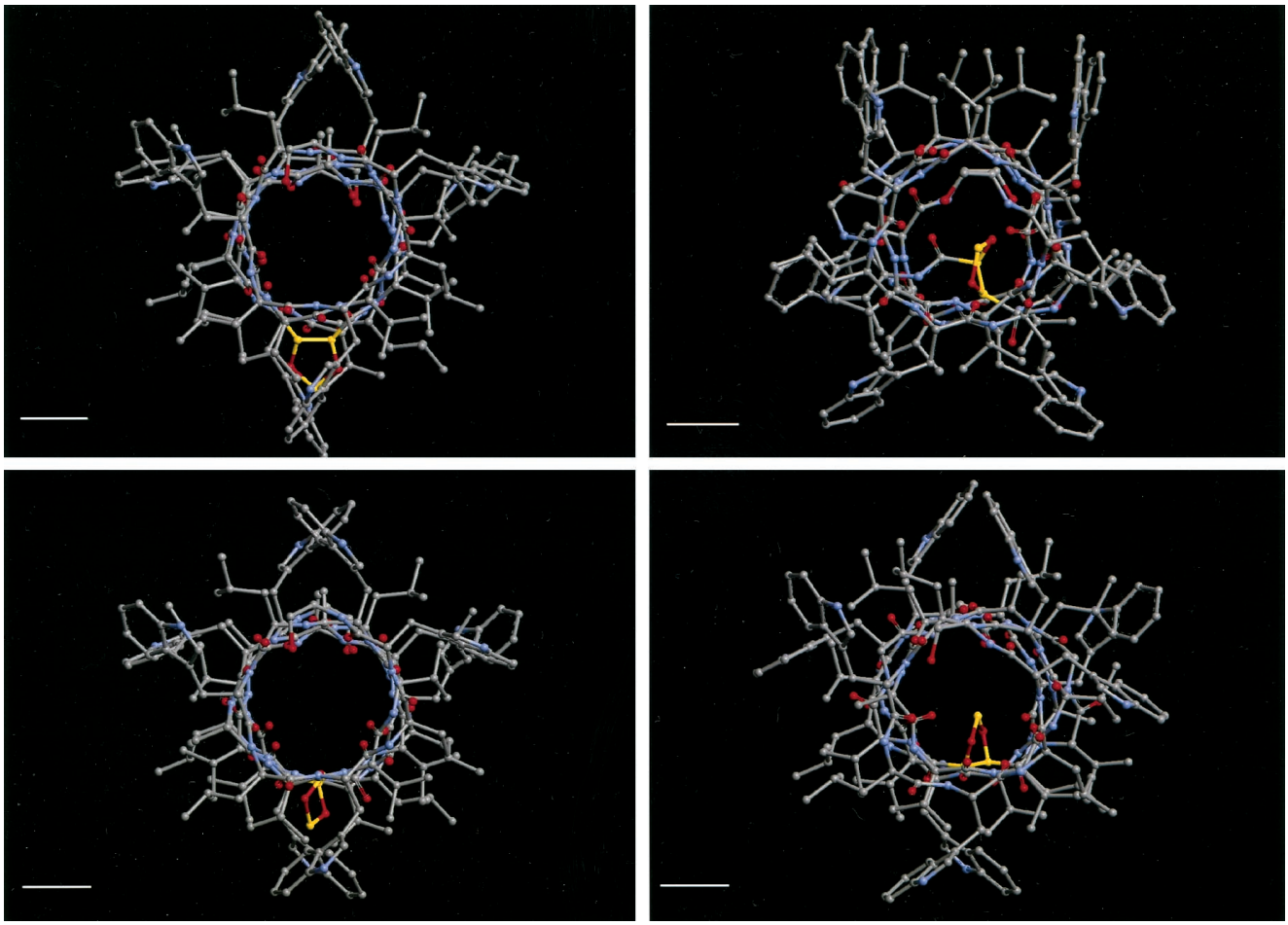

FIGURE 2 Cross-sectional views of the pore of the SS and RR dimers. The upper row shows the SS dimer with the dioxolane linker outside (SS-exo, *left*) and inside (SS-endo, *right*) the pore. The lower row shows the RR-exo (*left*) and RR-endo (*right*). The carbons of the dioxolane linker are identified in yellow. The calibration mark in each panel represents 3 Å. See text for discussion.

dioxolane ring is nearly perpendicular to that of the SS, whereas the overall pore diameter is essentially unchanged. However, and as discussed in relation to Fig. 1 and Table 1, the orientations of carbonyls are different between the SS-exo and RR-exo. This observation is significant because proton transfer in these dimers is markedly different (see below). Evidently, the distribution and orientation of carbonyls have a far more significant impact on proton transfer than the diameter of the pore itself.

The two right panels in Fig. 2 demonstrate the peptide distortion caused by rotating the respective SS and RR dioxolane rings into the lumen of the channel. This has been suggested to be the mechanism for channel closures in dioxolane-linked dimers (Stankovic et al., 1989). By rotating multiple ϕ-ψ angles and leaving peptide bonds planar, as described in Materials and Methods, it is possible for the linker to protrude inside the pore lumen. In this process, the RR dimer required less peptide reorganization than in the SS. In the RR, much of the distortion was at the interface, with carbonyls directed into the lumen. In the SS, considerably more rotation was required to reestablish some measure of helicity in the protein. Note that the carbonyls in the upper right panel that are approximately orthogonal to the axis of the channel project into the lipid bilayer.

Fig. 3 shows single-channel *I-V* plots of the SS and RR dimers reconstituted in PEPC bilayers in 1 M $[H^+]_{bulk}$. The RR has a significantly lower g_H than the SS dimer (Table 2). Linear portions of the *I-V* plot in Fig. 4 have a g_H of 516 and 228 pS for the SS and RR dimers, respectively. In the SS dimer, the *I-V* plot becomes sublinear around 100 mV at that proton concentration (Cukierman et al., 1997; Quigley et al., 1998). In contrast, the *I-V* relationship in the RR dimer is clearly supralinear in that same voltage range, as shown in the bottom panel of Fig. 3.

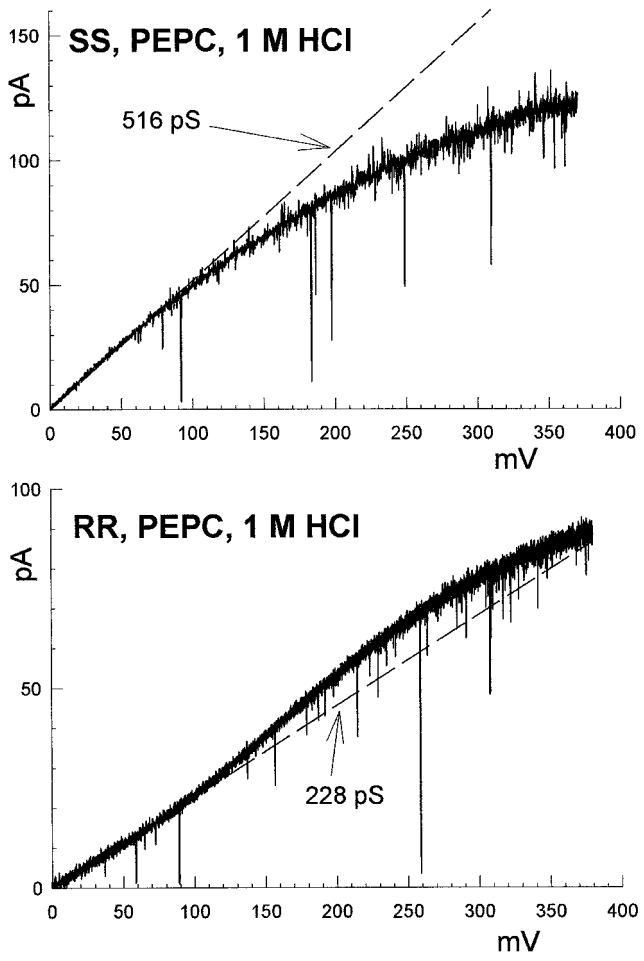

FIGURE 3 Single-channel *I-V* plots in response to voltage ramps applied to SS and RR dimers in PEPC (1 M HCl). Dashed lines represent the linear part of the g_H. Recordings were low-pass filtered at 2 kHz. Note single-channel closures in both recordings.

In Fig. 4, a continuous recording of a single SS dimer in PEPC at a transmembrane potential of 60 mV is shown. The typical lifetime of a SS dimer in lipid bilayers is determined essentially either by the duration of the experiment or by the lifetime of the bilayer (Cukierman et al., 1997; Quigley et al., 1998). In the specific case of Fig. 4, this single SS dimer lasted for the entire duration of the experiment (~70 min). We have conducted experiments in which the SS dimer remained stable in the bilayer for over 2 h. The SS dimer gates with very rapid, not completely resolved closures, even at recording frequencies of 10 kHz (Cukierman et al., 1997).

Fig. 5 shows a typical continuous recording of an RR dimer in a PEPC bilayer at a transmembrane potential of 50 mV. In this recording, the RR channel was incorporated into the bilayer a few seconds (time necessary to activate the videotape recorder) before the start of this recording. In contrast to what was mentioned before in relation to Fig. 4 (SS dimer), the RR dimer showed relatively long duration closures, and typically, the channel "disappeared" from the bilayer, as shown at the end of recording in Fig. 5. The disappearance (no channel opening observed within 1 min) of the RR channel from the bilayer will be referred to as inactivation. Sometimes the channel "reappeared" several minutes later in the bilayer. Evidently, it is not possible to ascertain whether it is the same or a different RR channel that was incorporated into the bilayer. Because of its limited lifetime in the bilayer, dwell-time distributions of fast closed states of the RR channel could not have been determined (small number of closing events).

Because 1) gA dimers have different single-channel properties in different lipid bilayers (Cukierman et al., 1997) and 2) the RR and SS dimers were previously studied in HCl solutions in GMO bilayers (Stankovic et al., 1989, 1990), it was of interest to perform experiments in GMO bilayers. In Fig. 6, *I-V* plots of the SS and RR dimers are shown in two different $[H^+]_{bulk}$. As with PEPC bilayers, g_H in the RR is significantly smaller than in the SS dimer. In 122 mM $[H^+]_{bulk}$, the single-channel conductances were 172 and 54 pS for the SS and RR dimers, respectively. In 1 M $[H^+]_{bulk}$, g_H's were 828 and 328 pS (Table 2). Contrary to what is shown for PEPC bilayers, there were no major differences in the shape of *I-V* plots between the SS and RR dimers in GMO bilayers.

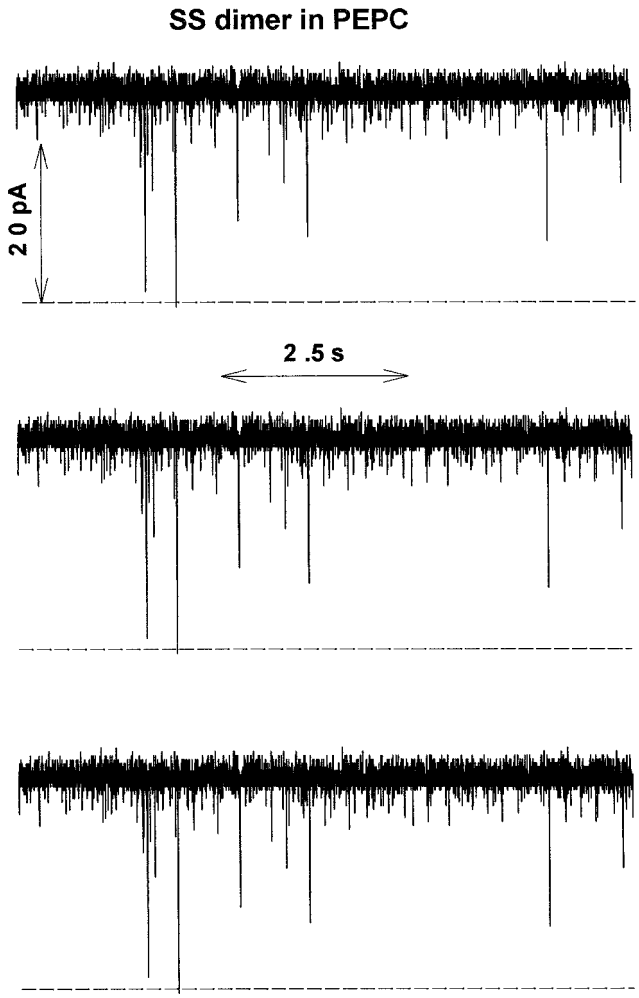

FIGURE 4 Continuous recording of a single-channel SS dimer in a PEPC bilayer at a membrane potential of 60 mV (1 M HCl). The recording was low-pass filtered at 1 kHz and sampled at 4 kHz.

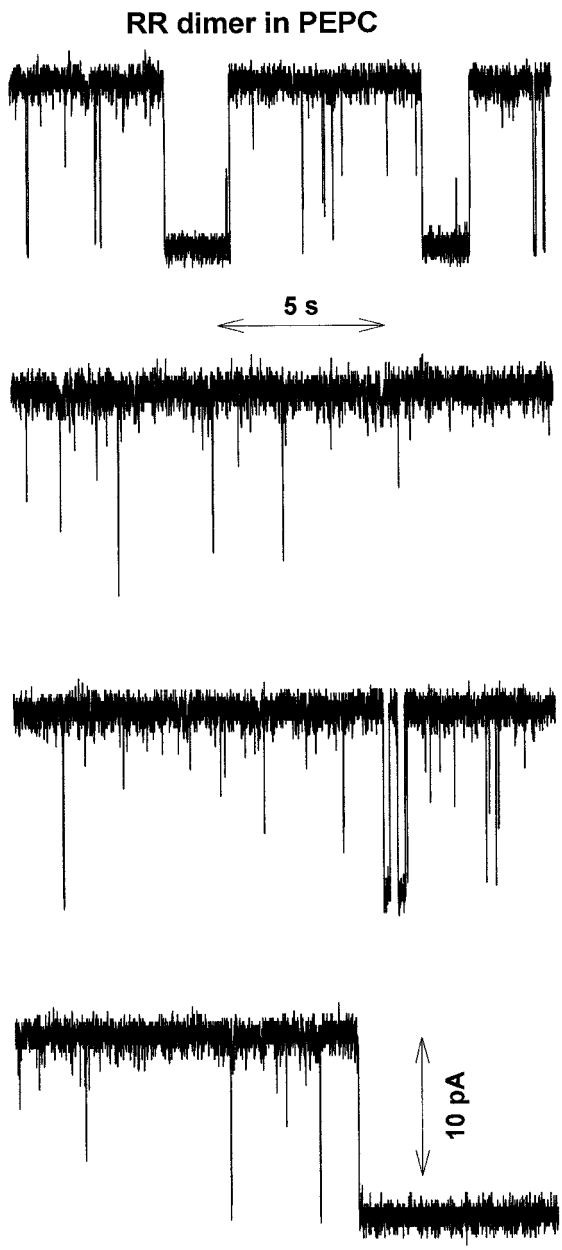

FIGURE 5 Continuous recording of single channel proton currents in the RR dimer in a PEPC bilayer at a transmembrane potential of 50 mV (1 M HCl). The recording was low-pass filtered at 1 kHz and sampled at 4 kHz. The end of the recording in the lower panel identifies the "inactivation" of the channel.

In 1 M $[H^+]_{bulk}$, the proton concentration at the PEPC/solution interface is 122 mM (see discussion of the underlying assumptions in Materials and Methods). g_H's (for both the SS and RR dimers) in GMO in 122 mM $[H^+]_{bulk}$ are considerably smaller than in PEPC with 1 M $[H^+]_{bulk}$ (Table 2).

Figs. 7 and 8 show continuous recordings in GMO bilayers of the SS and RR dimers, respectively. In Fig. 7, a single SS dimer was recorded in 2 M HCl at a transmembrane potential of 100 mV. The stable recording of the single-channel activity is characterized by fast flickers to the closed state as shown in Fig. 4. In Fig. 8, a single RR dimer was recorded in a 1 M HCl solution at 50 mV. Short-duration closures were also observed as with the SS dimer. However, RR channels were inactivated, as discussed before in relation to Fig. 5. The RR channel shown in Fig. 8 lasted ~90 s in the bilayer. The gatings of the SS and RR channels were qualitatively similar in the GMO and PEPC bilayers.

DISCUSSION

The novel findings reported in this study are: 1) g_H in the SS dimer is significantly larger than in the RR dimer; 2) shapes of *I-V* plots in PEPC (but not in GMO) bilayers are different between the SS and RR dimers; 3) the open state of the SS channel is stable, whereas the RR dimer eventually inactivates into a long-lasting closed state. Based on single-channel properties in different experimental conditions, it is concluded that our previously studied D_1 dimer (Cukierman et al., 1997; Quigley et al., 1998) is indeed the SS dioxolane

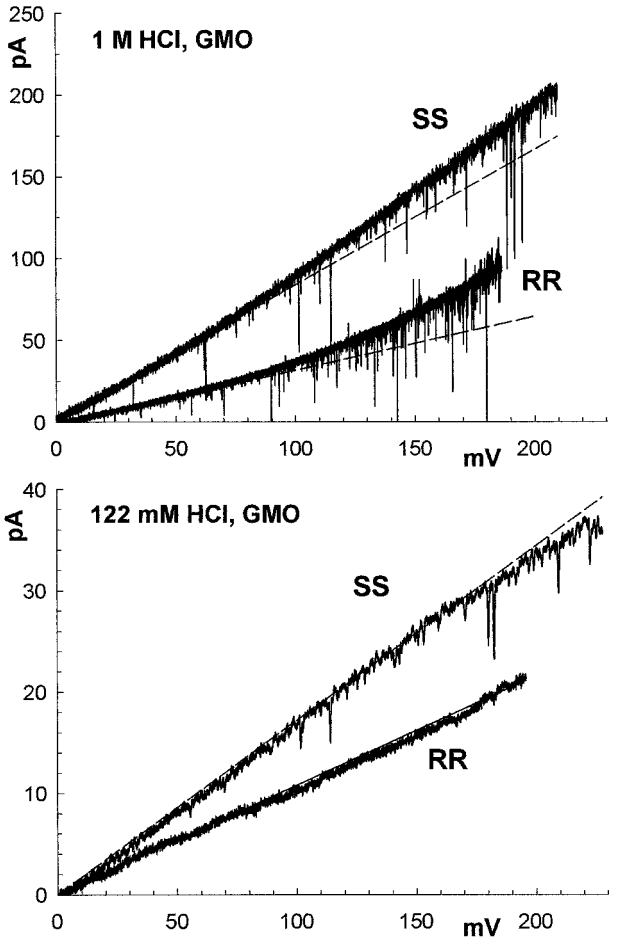

FIGURE 6 Single-channel *I-V* plots in response to voltage ramps applied to SS and RR dimers in GMO under different HCl concentrations. Dashed lines represent single-channel conductances of 828 and 328 pS (*upper recordings*), and 172 and two channels of 54 pS each (*lower recordings*). Single-channel recordings were low-pass filtered at 1 kHz (*upper recording*) and 300 Hz (*lower recording*).

linked dimer. In addition, differences between the H-bonding pattern in the RR and SS dimers modeled in this study could account for the observed differences in g_H between these channels.

Single-channel proton conductance in different gA dimers and bilayers

Proton transfer in water

The transfer of protons in a H-bonded chain of water molecules (water wire) is a two-step process (Bernal and Fowler, 1933). First, a proton hops in a given direction between two adjacent water molecules. This causes a complete reorganization of H-bonds between these two water molecules. A sequence of proton hops along the water wire causes a complete rearrangement of H-bonds and covalent bonds inside that water chain. In this new configuration, the water wire cannot conduct protons in the same direction. The second step comprises rotations of water molecules in

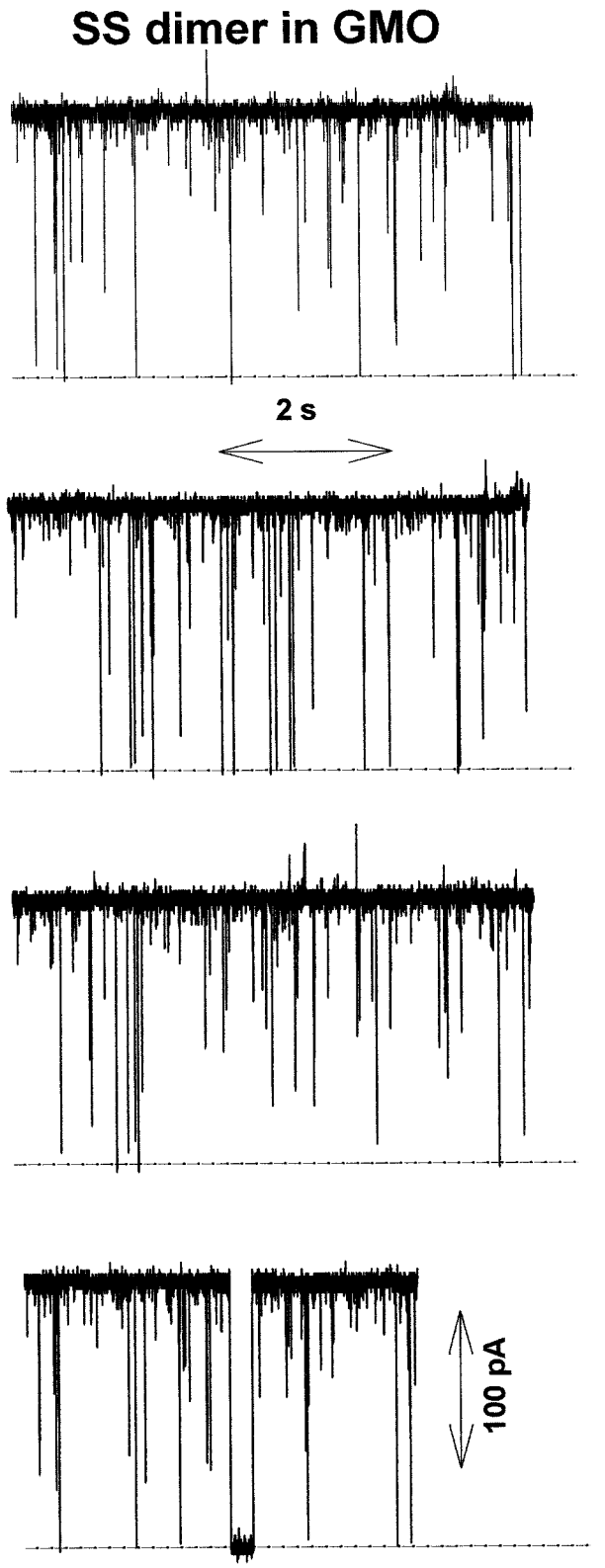

FIGURE 7 Continuous recording of single-channel proton currents in the SS dimer in a GMO bilayer at a transmembrane potential of 100 mV (2 M HCl). The recording was low-pass filtered at 4 kHz, sampled at 4 kHz, and decimated.

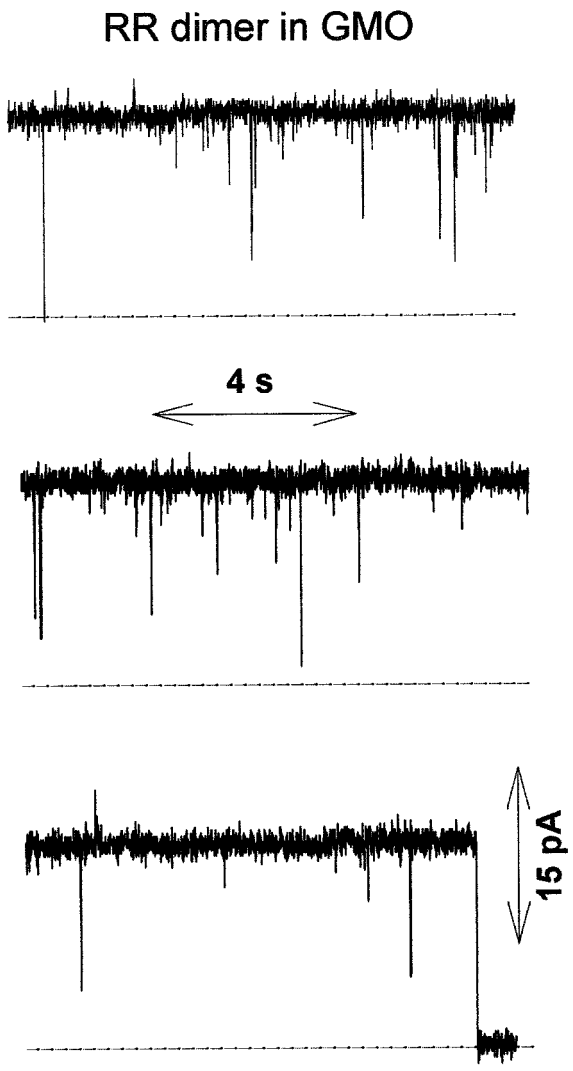

FIGURE 8 Continuous recording of single-channel proton currents in the RR dimer in a GMO bilayer at a transmembrane potential of 50 mV (1 M HCl). The recording was low-pass filtered at 1 kHz, sampled at 2 kHz, and decimated.

a H-bonded water chain. These rotations prime the chain of H-bonded waters back to the initial configuration, and only then can a different proton be transferred in the same direction along the water wire. These mechanisms (proton hopping and water reorientation) can explain the relatively high proton mobility in water (Agmon, 1995, 1996; Bernal and Fowler, 1933; Pomès and Roux, 1998). Because this model (popularly known as the Grotthuss mechanism) was proposed, the rate-limiting step in proton transfer in water has been attributed to the turn step, i.e., the reorientation of water molecules in the water wire is considerably slower than proton hopping (see Pomès and Roux, 1998). It should be noticed that a careful reinterpretation of proton transfer in bulk water was recently proposed (Agmon, 1995, 1996; Tuckerman et al., 1995). The rate-limiting step in proton transfer between water molecule complexes is the cleavage of an ordinary H-bond (2.6 kcal/mol) in the second solvation shell of $(H_3O)^+$. Once this H-bond is broken, proton transfer within $(H_5O_2)^+$ complexes becomes an activationless process (Agmon, 1996).

Proton transfer in gA channels

The large single-channel conductance of protons in relation to other monovalent cations in gA channels has been known for a long time (Akeson and Deamer, 1991; Cukierman et al., 1997; Eisenman et al., 1976; Heinemann, 1990; Hladky and Haydon, 1972; Levitt and Decker, 1988; Myers and Haydon, 1972). This led to the proposal and demonstration that protons cross gA channels via a Grotthuss-like mechanism (Levitt et al., 1978; Pomès and Roux, 1996). The single-channel proton conductance in the SS dimer is also very large in relation to other monovalent cations (Cukierman et al., 1997). Indeed, the mobility of protons in the SS dimer is comparable to their mobility in HCl solutions (Cukierman, 1999).

The translocation of a H^+ along a single file of water molecules inside the gA pore in the absence of an applied electric field was recently studied using molecular dynamics simulations (Pomès and Roux, 1996). The presence of an extra proton in the pore caused a change in the orientation of water molecules and in their H-bond interactions. Proton transfer between adjacent water molecules occurred spontaneously in the sub-picosecond time scale. The transfer of one proton across a significant length of the channel occurred in several picoseconds. Because the time residency of a proton inside the SS dimer can be on the order of 10^3 ps (Cukierman, 1999), it is likely that the rate-limiting step in proton transfer in gA must reside in the reorganization of the H-bond network between waters inside the pore and the carbonyl groups lining the pore. Indeed, proton transfer across the pore occurred at a considerably faster rate when water molecules were not allowed to interact electrostatically with the channel wall (Pomès and Roux, 1996). Consequently, electrostatic interactions between water and channel carbonyls would have the effect of retarding the reorientation of water molecules inside the pore, thus decreasing H^+ transport.

Modulation of proton conduction in gA channels: implications for proton transfer in proteins

Differences in proton conduction between the SS and RR dimers. It is concluded from the discussion above that the rate of proton transfer in the SS or RR dimers should ultimately depend on the overall H-bond interactions between water molecules and the wall of the channel. Such interactions would determine the relative distribution and orientation of H_2O molecules inside the pore. Our results have clearly demonstrated that g_H in the RR dimer is considerably smaller than in the SS channel. Evidently, the distribution and/or reorientation dynamics of H_2O molecules inside the pore of the channel must be significantly different between the SS and RR dimers. This is the func-

tional consequence of the marked structural differences between the RR and SS dimers. For example, stronger H-bond interactions between water molecules and carbonyls in the RR in relation to the SS dimer could account for a lower g_H in the RR dimer by hampering the reorientation of water molecules inside the pore (Pomès and Roux, 1996). Indeed, Table 1 showed that H-bonds between the residues of the SS and RR dimers are different in number and geometries. In the RR, one H-bond is missing in relation to the SS dimer. Other H-bonds, as evaluated by their geometries, could be potentially weaker in the RR than in the SS dimer. It is conceivable that some extra (in number and/or energetics) H-bonds between water and the channel wall could exist in the RR in relation to the SS dimer. This would have the effect of reducing the probability of water reorientation required for fast proton transfer, thus attenuating g_H.

In conclusion, there is a basic conceptual justification of the experimental finding that different stereoisomers of the dioxolane-linked dimers have different single-channel conductances to protons. Obviously, the methodology used in this study does not allow the identification of the precise atomic mechanisms responsible for different g_H's in the SS and RR dimers. Nevertheless, our single-channel measurements and molecular modeling suggest that qualitative and quantitative differences in H-bond interactions between water and channel wall in the SS and RR dimers may well underlie the different g_H's measured in these channels.

The linear portion of *I-V* plots was not the only difference between the SS and RR dimers. *I-V* plots of the SS and RR dimers were qualitatively similar in GMO bilayers. In PEPC bilayers, however, *I-V* plots were sublinear for the SS (Cukierman et al., 1997; Quigley et al., 1998) and supralinear (S-shaped) for the RR dimer (Fig. 3). If proton permeation through a dimer channel is viewed as a sequence of independent, voltage-dependent kinetic steps following transition state rate theory, some qualitative insights can be gained. The supralinearity in the RR dimer could then be seen as a consequence of a steep voltage-dependent kinetic step inside the channel's pore that is absent in the SS dimer. Indeed, it was not difficult to model the different *I-V* shapes of the SS and RR dimers with this strategy (results not shown). On the other hand, the sublinearity of the SS dimer in a PEPC bilayer suggests that a kinetic step is poorly voltage dependent. The rate of proton transfer through the SS channel is comparable to the proton mobility in HCl solutions (Cukierman, 1999). This means that at relatively high voltages and low $[H^+]$, g_H may be limited by the flow of protons from bulk solution to the mouths of the pore and vice versa. Therefore, diffusion limitation can cause sublinearity of *I-V* plots in relatively low ionic concentrations (Akeson and Deamer, 1991; Andersen, 1983). In Fig. 3, sublinearity (in the SS dimer) and supralinearity (in the RR dimer) overlap over a considerable range of voltage and current values. These differences between *I-V* plots of the SS and RR dimers in PEPC bilayers (Fig. 3) make diffusion limitation unlikely to be the only or major factor underlying the sublinearity of the SS dimer. Moreover, *I-V* plots of a given gA dimer are different in phospholipid and GMO bilayers (Busath et al., 1998; Cukierman et al., 1997). Thus diffusion limitation may not be the main or sole factor in the sublinearity of the SS dimer. Although we are not yet in a position to provide a complete model of *I-V* plots of different gA dimers, the general idea that water dynamics as related to proton transfer inside the pore of gA channels is the major determinant of the characteristics of the *I-V* plot is favored (Cukierman et al., 1997).

In our experimental conditions, PEPC bilayers are positively charged, whereas GMO is neutral. A $[H^+]_{bulk}$ of 1 M corresponds to 122 mM at the PEPC/solution interface ($[H^+]_{x=0}$; see Cukierman, 1991; Cukierman et al., 1997; and Materials and Methods for a discussion on important limitations of this approximate calculation). The mouths of the gA dimer are likely to see this "corrected" $[H^+]_{x=0}$ instead of $[H^+]_{bulk}$. It was previously found that g_H in the SS dimer in PEPC bilayers is significantly larger than in GMO bilayers when $[H^+]_{x=0}$ was used as the proton concentration (Cukierman et al., 1997). This observation is now extended to the RR dimer. Note that g_H in GMO at 122 mM is 47 pS, whereas in 1 M $[H^+]_{bulk}$ PEPC ($[H^+]_{x=0}$ ~122 mM) it is 232 pS. Because g_H at a given $[H^+]_{x=0}$ is larger in PEPC than in GMO bilayers, it is possible that an extra source of protons for permeation through the RR dimer must be available in PEPC bilayers that is not present in GMO bilayers. In GMO bilayers the only source of protons for permeation in the SS dimer is the bulk solution. During proton conduction through the RR dimer, proton depletion at the channel's mouth must occur. This would have the effect of limiting the single-channel proton current. In PEPC (but not in GMO) bilayers, proton depletion at the channel's entrance would promote deprotonation of phospholipids close to the mouth of the RR dimer. This could be the additional source of H^+ for channel permeation. Such a mechanism could work if reprotonation of phospholipids close to the mouth of the pore via adjacent phospholipids in the lipid monolayer occurs by a faster process than reprotonation of phospholipids via proton diffusion from bulk solution. It has been proposed that proton mobility along a phospholipid monolayer is considerably faster than in bulk solution (see Antonenko and Pohl, 1998; Gutman et al., 1995; Haines, 1983; Teissie et al., 1985), and this could account for the fast reprotonation of phospholipids close to the mouth of the SS dimer.

Interfacial dipole potentials and g_H. Even though the large single-channel conductance to protons in gA channels has been known for a long time (see references in Introduction), only in very recent years have we started to address the molecular mechanisms underlying g_H (Pomès and Roux, 1996). The recent study by Phillips et al. (1999) complements and is of special interest to the experimental findings described here. Those authors found that fluorination of Trp side chains in natural gA channels attenuated g_H. Conversely, replacement of Trp by Phe enhanced g_H. These experimental results were explained by an elegant model in which water reorientation (the rate-limiting step in proton

translocation along gA channels; see above) at the channel's ends is strongly affected by the interfacial dipole potential (IDP). The IDP in the monolayer on the side of the membrane where protons exit the channel has the same orientation as the total dipole moment of the chain of water molecules ready to transport protons. IDP modulates the reorientation of water molecules located at the end of the pore, where H^+ leaves the channel (see figure 7 in Phillips et al., 1999). Fluorination of Trp (or replacement of Trp by Phe) at that end of the channel pore would decrease (or increase) g_H by decreasing (or increasing) the IDP. Although this proposed mechanism may not explain the differences in g_H between the SS and RR dimers, it offers an important additional paradigm that furthers our understanding of molecular mechanisms by which proton transport could be modulated in proteins.

Another experimental result in the study by Phillips et al. (1999) that is of relevance to our observations is that those authors found that g_H in a diphytanoyl PC bilayer is larger than in a GMO bilayer at a given $[H^+]_{bulk}$ (not corrected for protonation and surface charge effects of the phospholipid). That result is the opposite of what we described for PEPC and GMO bilayers (Cukierman et al., 1997; Quigley et al., 1998; see first and second lines in Table 2). Some preliminary results from our laboratory (Cukierman, unpublished observations) have demonstrated that there are differences in single-channel conductance and gating in PC versus PEPC bilayers. The different experimental results obtained by us and by Phillips et al. (1999) will be addressed in the near future. The study of those differences should further our understanding of medium-range and long-range effects on proton conduction in gA channels.

Gating of the SS and RR dimers

The pioneering work of Stankovic et al. (1989, 1990) revealed that the SS dimer remained essentially in the open configuration, whereas the RR dimer showed fast closing events. These results were obtained in different solutions (KCl or HCl). Molecular dynamics simulations (Crouzy et al., 1994) showed that in both the SS and RR dimers, the lowest energy minimum is attained when the dioxolane link is outside the pore (Fig. 2, *left panels*). In the RR dimer there is an energetically favorable path for the dioxolane to move from outside of to inside the pore in a sequence of different chemical steps (Fig. 2, *bottom row*). In contrast, this movement in the SS dimer is energetically more costly but clearly not impossible (see Crouzy et al., 1994). The H-bonded chain of water molecules inside the pore of the dimers is interrupted when the dioxolane link is inside the pore. This means that H^+ transfer can no longer occur along the water wire. Consequently, the fast flickers that were only observed in the RR by Stankovic et al. (1989, 1990), and in our experiments with both the SS and RR dimers, could be explained by the movement of the dioxolane linker into the pore. Although Crouzy et al. (1994) favored that said movement would occur in the RR dimer only, those authors acknowledged the possibility that different kinetics could occur in different lipid environments, and with different (qualitative and/or quantitative) ions inside the pore of dioxolane-linked dimers. Because in our experimental conditions, the open state of natural gA channels lacks the fast closures seen with gA dimers (Cukierman et al., 1997), fast closing flickers in both the RR and SS dimers must be directly or indirectly (see below) related to the presence of the dioxolane linker in these molecules.

Fast closures were also noticed in gA channels without dioxolane linkers. For example, carbon suboxide-linked gA channels have fast closing events during the long openings of the channel (Bamberg and Janko, 1977). Fast closures in natural gA channels in lipid bilayers have also been demonstrated (Ring, 1986). Following the discussion above, it is possible that the reorganization of H-bonds in the peptide backbone affects the dynamics of water molecules inside the pore, causing interruptions in H^+ transfer (seen as channel closures). An important factor to consider is that the dynamic flexibility of the helical chain of gA affects the mobility of waters inside the pore (Chiu et al., 1991). This could also modulate proton transfer and gating in gA channels.

Experimental results of this study clearly demonstrated that both the SS and RR dimers have fast closing events in either GMO or PEPC bilayers. Moreover, it was noticed that the RR dimer "inactivates." Thus, whereas the SS dimer gating is consistent with a simple O (open) $\leftrightarrow$ C (closed) kinetic scheme (Cukierman et al., 1997), gating in the RR is more complex, with an additional inactivated (I) state (I $\leftrightarrow$ C $\leftrightarrow$ O $\leftrightarrow$ I). It is not clear what is causing inactivation in the RR dimer. One possibility is that there is a very stable conformation of the dioxolane linker inside the RR dimer, interrupting the water chain for prolonged times. Another possibility could be a more dramatic conformational change of the entire protein structure of the RR dimer, resulting in the disappearance of channel activity.

Comparison with previous experimental results

It has been reported (Stankovic et al., 1990) that g_H in different dioxolane linked dimers was nearly the same in 40 mM HCl. It was also reported that the SS dimer remains in the open state essentially 100% of the time, whereas the RR dimer showed fast closing events. The results described in this paper are not in agreement with those experimental findings. The only methodological difference between our studies is that we have used the planar bilayer system, whereas Stankovic and colleagues formed bilayers at the tip of a glass pipette. Bilayers at the pipette tip can be under tension (Heinemann, 1990). The extent to which the behavior of dioxolane-linked gA dimers is affected by tension (as with natural gA channels; see Lundbæk et al., 1997) is an interesting topic for future development.

Previous work from our own laboratory (Cukierman et al., 1997; Quigley et al., 1998) have used the product of dimerization reaction from an initial racemic mixture of D-

and L-tartaric acids. Both RR and SS dimers, unequivocally individualized in the present study by their long open times, were seen in previous experiments. We can now conclude that 1) The previously designated D_1 (or gA~D_1~gA) channel is the SS dimer. 2) A channel designated as gA~D_2~gA (or D_2) was identified in our lipid bilayers. This channel has a gating behavior completely different from that of the RR or SS channels. D_2 channels are in the closed state most of the time and have brief openings and a short lifetime in lipid bilayers. D_2 channels were also infrequently seen (as before) in experiments with solutions containing the pure SS or RR dimer. Is it possible that D_2 channels represent a different conformation of dioxolane-linked dimers?

We thank Dr. Lothar Blatter for his help in preparing Figs. 1 and 2. We are grateful to Dr Régis Pomès for discussions on energy minimization protocols in proteins, and for his thorough deconstruction of a previous version of the manuscript. Many thanks also to Dr. David D. Busath for providing us with unpublished material, and for insightful discussions on proton transport in water wires.

EPQ was supported by a Schmitt Fellowship from the Graduate School of Loyola University Chicago.

REFERENCES

Agmon, N. 1996. Hydrogen bonds, water rotation and proton mobility. *J. Chim. Phys.* 93:1714–1736.

Akeson, M., and D. W. Deamer. 1991. Proton conductance by the gramicidin water wire. Model for proton conductance in the F_0F_1 ATPases? *Biophys. J.* 60:101–109.

Andersen, O. S. 1983. Ion movement through gramicidin A channels. Single channel measurements at very high potentials. *Biophys. J.* 41: 119–133.

Antonenko, Y. N., and P. Pohl. 1998. Coupling of proton source and sink via H^+-migration along the membrane surface as revealed by double patch-clamp experiments. *FEBS Lett.* 429:197–200.

Arseniev, A. S., I. L. Barsukov, V. F. Bystrov, A. L. Lonize, and Y. A. Ovchinikov. 1985. Proton NMR study of gramicidin A transmembrane ion channel. Head-to-head right handed, single stranded helices. *FEBS Lett.* 186:168–174.

Baciou, L., and H. Michel. 1995. Interruption of the water chain in the reaction center from rb. sphaeroides reduces the rate of the proton uptake and of the second electron transfer to Q B. *Biochemistry*. 34: 7967–7972.

Bamberg, E., and K. Janko. 1977. The action of a carbonsuboxide dimerized gramicidin A on lipid bilayer membranes. *Biochim. Biophys. Acta.* 465:486–499.

Bernal, J. D., and R. H. Fowler. 1933. A theory of water and ionic solution, with particular reference to hydrogen and hydroxyl ions. *J. Chem. Phys.* 1:515–548.

Busath, D. D., C. D. Thulin, R. W. Hendershot, L. R. Phillips, P. Maughan, C. D. Cole, N. C. Bingham, S. Morrison, L. C. Baird, R. J. Hendershot, M. Cotten, and T. A. Cross. 1998. Noncontact dipole effects on channel permeation. I. Experiments with (5F-indole) Trp^{13} gramicidin A channels. *Biophys. J.* 75:2830–2844.

Chiu, S. W., E. Jakobsson, S. Subramaniam, and J. A. McCammon. 1991. Time-correlation analysis of simulated water motion in flexible and rigid gramicidin channels. *Biophys. J.* 60:273–285.

Crouzy, S., T. B. Woolf, and B. Roux. 1994. A molecular dynamics study of gating in dioxolane-linked gramicidin A channels. *Biophys. J.* 67: 1370–1386.

Cukierman, S. 1991. Asymmetric electrostatic effects on the gating of rat brain sodium channels in planar lipid membranes. *Biophys. J.* 61: 845–856.

Cukierman, S. 1999. Flying protons in linked gramicidin A channels. *Isr. J. Chem.* (in press).

Cukierman, S., E. P. Quigley, and D. S. Crumrine. 1997. Proton conduction in gramicidin A and in its dioxolane-linked dimer in different lipid bilayers. *Biophys. J.* 73:2489–2502.

Deamer, D. W., and J. W. Nichols. 1989. Proton flux mechanisms in model and biological membranes. *J. Membr. Biol.* 107:91–103.

DeCoursey, T. E., and V. V. Cherny. 1994. Voltage-activated hydrogen ion currents. *J. Membr. Biol.* 141:203–223.

DeCoursey, T. T., and V. Cherny. 1999. An electrophysiological comparison of voltage-gated proton channels, other ion channels, and other proton channels. *Isr. J. Chem.* (in press).

Eisenman, G., B. Enos, J. Hägglund, and J. Sandblom. 1980. Gramicidin as an example of a single-filing ionic channel. *Ann. N.Y. Acad. Sci.* 339: 8–20.

Gutman, M., E. Nachliel, and Y. Tsfadia. 1995. Propagation of protons at the water membrane interface. Microscopic evaluation of a macroscopic process. *In* Permeability and Stability. E. A. Disalvo and S. A. Simon, editors. CRC Press, Boca Raton, FL. 259–276.

Haines, T. H. 1983. Anionic lipid headgroups as a proton-conducting pathway along the surface of membranes: a hypothesis. *Proc. Natl. Acad. Sci. USA.* 80:160–164.

Heinemann, S. H. 1990. Untersuchung interner bewegungen von kanalbildenden proteinen mit elektophysiologischen methoden und kraftfeldrechnungen. Dissertation. University of Gottingen, Gottingen.

Hladky, S. B., and D. A. Haydon. 1972. Ion transfer across lipid membranes in the presence of gramicidin A. I. Studies of the unit conductance channel. *Biochim. Biophys. Acta.* 274:294–312.

Ketchem, R. R., W. Hu, and T. A. Cross. 1993. High resolution of gramicidin A in a lipid bilayer by solid-state NMR. *Science.* 261: 1457–1460.

Koeppe, R. E., II, and O. S. Andersen. 1996. Engineering the gramicidin channel. *Annu. Rev. Biophys. Biomol. Struct.* 25:231–258.

Levitt, D. G., and E. R. Decker. 1988. Electrostatic radius of the gramicidin channel determined from voltage dependence of H^+ ion conductance. *Biophys. J.* 53:33–38.

Levitt, D. G., S. R. Elias, and J. M. Hautman. 1978. Number of water molecules coupled to the transport of sodium, potassium, and hydrogen ions via gramicidin nonactin or valinomycin. *Biochim. Biophys. Acta.* 512:436–451.

Lundbæk, J. A., A. M. Maer, and O. S. Andersen. 1997. Lipid bilayer electrostatic energy, curvature stress, and assembly of gramicidin channels. *Biochemistry.* 36:5695–5701.

Myers, V. B., and D. A. Haydon. 1972. Ion transfer across lipid membranes in the presence of gramicidin A. *Biochim. Biophys. Acta.* 274:313–322.

Oliver, A. E., and D. W. Deamer. 1994. α-Helical hydrophobic polypeptides form proton-selective channels in lipid bilayers. *Biophys. J.* 66: 1364–1379.

Phillips, L. R., C. D. Cole, R. J. Hendershot, M. Cotten, T. A. Cross, and D. D. Busath. 1999. Non-contact dipole effects on channel permeation. III. Anomalous proton conductance effects in gramicidin. *Biophys. J.* 77:2492–2501.

Pomès, R., and B. Roux. 1996. Structure and dynamics of a proton wire: a theoretical study of H^+ translocation along the single-file water chain in the gramicidin A channel. *Biophys. J.* 71:19–39.

Pomès, R., and B. Roux. 1998. Free energy profiles for H^+ conduction along hydrogen-bonded chains of water molecules. *Biophys. J.* 75: 33–40.

Quigley, E. P., A. Emerick, D. S. Crumrine, and S. Cukierman. 1998. Proton current attenuation by methanol in a dioxolane-linked gramicidin A dimer in different lipid bilayers. *Biophys. J.* 5:2811–2820.

Riistma, S., G. Hummer, A. Puustinem, R. B. Dyer, W. H. Woodruff, and M. Wilkström. 1997. Bound water in the proton translocation mechanism of the heme-copper oxidases. *FEBS Lett.* 414:275–280.

Ring, A. 1986. Brief closures of gramicidin A channels in lipid bilayer membranes. *Biochim. Biophys. Acta.* 856:646–653.

Stankovic, C. J., S. H. Heinemann, J. M. Delfino, F. J. Sigworth, and S. L. Schreiber. 1989. Transmembrane channels based on tartaric acid-gramicidin A hybrids. *Science.* 244:813–817.

Stankovic, C. J., S. H. Heinemann, and S. L. Schreiber. 1990. Immobilizing the gate of a tartaric acid-gramicidin A hybrid channel molecule by rational design. *J. Am. Chem. Soc.* 112:3702–3704.

Teissie, J., M. Prats, P. Soucaille, and J. F. Tocanne. 1985. Evidence for conduction of protons along the interface between water and a polar lipid monolayer. *Proc. Natl. Acad. Sci. USA.* 82:3217–3221.

Tuckerman, M., K. Laasonen, M. Sprik, and M. Parinello. 1995. *Ab initio* molecular dynamics simulation of the solvation and transport of H_3O^+ and OH^- ions in water. *J. Phys. Chem.* 99:5749–5752.